Soft Matter

Cite this: *Soft Matter*, 2011, **7**, 10274

www.rsc.org/softmatter

PAPER

Probing protein conformations at the oil droplet–water interface using single-molecule force spectroscopy

Ahmed Touhami,[abc] Marcela Alexander,[d] Martin Kurylowicz,[ab] Colin Gram,[a] Milena Corredig[d] and John R. Dutcher*[ab]

Received 7th July 2011, Accepted 23rd August 2011
DOI: 10.1039/c1sm06284k

We have used atomic force microscopy (AFM) imaging and single molecule force spectroscopy (SMFS) to study β-lactoglobulin (β-LG) molecules localized at the interface between oil droplets and water. To immobilize the oil droplets, we have mechanically trapped them in the pores of a filtration membrane. For this sample geometry, we have used SMFS to pull on the β-LG molecules, revealing changes in their conformation and oligomerization in response to *in situ* changes in pH. We have compared the present results with those obtained previously for SMFS measurements of β-LG molecules adsorbed onto mica surfaces. At neutral pH, we observe large differences between the results obtained for the two surfaces in the pulling force required to fully extend the molecules, the spacing between sawtooth peaks in the force–distance curves, and the oligomerization of the molecules. The mechanical unfolding of the adsorbed β-LG molecules at pH 2.5 was very similar for the two surfaces. For pH 9.0, we find that, for both surfaces, there is an irreversible change in the conformation of the β-LG molecules with a strong repulsion measured between the AFM tip and the β-LG molecules. This study provides insight into structural changes of this protein when adsorbed onto an oil–water interface, and demonstrates the potential of SMFS as a tool to study the structure of proteins that are important in complex matrices such as food emulsions.

Introduction

Because of their amphiphilic character, many proteins tend to adsorb onto interfaces such as air–water, solid–water and oil–water.[1,2] Their surface-active behaviour has enormous implications in medicine, biotechnology and the food industry.[3,4] In general, the conformation of proteins changes upon adsorption to an interface: the protein molecules can spread out, or not, in response to various forces such as electrostatic and dispersion forces as well as hydrophilic and hydrophobic effects. For example, at an oil–water interface, the hydrophobic moieties of the proteins will tend to associate with the hydrophobic interface, changing the conformation to lower the free energy of the protein. Globular proteins such as whey proteins (more specifically, α-lactalbumin and β-lactoglobulin) are widely used as food ingredients because of their surface-activity and colloid-stabilizing properties.[2,5] During emulsion formation, the various protein molecules and aggregates become rapidly adsorbed at the surface of the newly formed oil droplets, forming layers that sterically and electrostatically stabilize the fine droplets.[6]

β-lactoglobulin (β-LG) is the predominant protein present in whey proteins, and plays a major role in determining the processing functionality of whey. For this reason, it has been extensively studied.[5] It is a small protein made of 162 amino acid residues (~18 kDa) whose structure is known from X-ray and NMR studies.[7–9] In solution, β-LG consists of two crossed β-sheets, each consisting of four β-strands, forming an open calyx structure, and an additional β-strand and one major α-helix. β-LG has two disulfide bridges and one free cysteine group. The inner faces of the β-sheets are hydrophobic, forming a hydrophobic cavity in the middle of the molecule. The inner cavity of the calyx can bind small hydrophobic molecules such as fatty acids for which it might act as a transporter.[10] In solution, β-LG exists as a dimer at neutral pH. As the pH is reduced below the isoelectric point pI = 5.2,[1] the number of charges increases such that below pH 3.5 the β-LG dimers dissociate into monomers while retaining their native conformation for pH values as low as 2.[11]

Because of the critical importance of the conformation of β-LG molecules to the stability of emulsions, many experimental studies have attempted to measure their conformation at the oil–water interface. FTIR spectroscopy has been the primary tool for these studies since it is possible to perform FTIR measurements on optically turbid emulsions.[12–15] These studies on β-LG

[a]*Department of Physics, University of Guelph, Guelph, Ontario, Canada N1G 2W1. E-mail: dutcher@uoguelph.ca; Fax: +519-836-9967; Tel: +519-824-4120, ext. 53950*
[b]*Advanced Foods and Materials Network – Networks of Centres of Excellence (AFMnet)*
[c]*Department of Physics & Astronomy, University of Texas at Brownsville, Brownsville, Texas, 78520, USA*
[d]*Department of Food Science, University of Guelph, Guelph, Ontario, Canada N1G 2W1*

stabilized oil-in-water emulsions suggested that there is a decrease in the β-sheet content with a corresponding increase in the α-helical content upon adsorption to the oil–water interface: however, there is some quantitative disagreement between the interpretation of the different measurements.

Circular dichroism (CD) is another standard optical technique for measuring the secondary structure of proteins in solution, but it is difficult to perform CD measurements on oil–water emulsions because the large index of refraction mismatch between the oil and water components of the emulsion gives rise to a large amount of background light scattering. Husband *et al.* addressed this problem by adding glycerol to achieve index-matching of the emulsions, rendering them optically clear, which allowed CD measurements to be performed.[13] For the index-matched emulsions, their CD results showed that there was a significant increase in the α-helical content upon adsorption to the oil–water interface. However, the FTIR measurements performed on the same index-matched samples gave a contradictory result: little change in the α-helical content, an increase in the β-turn structure, and essentially no change in the β-sheet structure. In these index-matched samples, a very high concentration of glycerol (58% by volume) was necessary to achieve index matching. This likely complicated the interpretation of the CD and FTIR data since glycerol can affect the conformation of the β-LG molecules by changing the hydration environment of the molecules.[16–18]

In another approach to evaluate the effect of interfacial adsorption on the conformation of β-LG molecules, Zhai *et al.* exploited the high signal-to-noise that is inherent to synchrotron-based CD to study emulsions that were not index-matched.[19] By subtracting CD spectra obtained from emulsions stabilized with a common nonchiral surfactant (SDS) from those obtained from emulsions stabilized with β-LG, they inferred the conformation of the adsorbed β-LG molecules. Although it is difficult to compare their structural element assignments with those of previous studies since their assignments did not account for a random coil component, they also reported that adsorption of the β-LG molecules to the oil–water interface resulted in a significant increase in α-helical content. Despite the considerable effort that has been invested with FTIR and CD to determine the secondary structure of β-LG molecules at the oil–water interface, the technical challenges involved in these measurements introduce some ambiguity into the determination of the secondary structure.

Recently, another technique based on atomic force microscopy (AFM) has been used to measure the conformation of proteins adsorbed onto an interface. Since its invention in the mid-1980s,[20] AFM has evolved from a high resolution imaging tool to a variety of techniques that allow detailed investigations of molecular forces at interfaces. Single-molecule force spectroscopy (SMFS) has been developed to manipulate single molecules, in real time and under physiological conditions, and is ideally suited to directly quantify the forces involved in both intra- and inter-molecular protein interactions. SMFS allows the direct measurement of the mechanical stability of the structure of proteins: by allowing the AFM tip to adhere to the protein molecule, it is possible to pull on the molecule, and forces as small as tens of piconewtons and changes in length as small as nanometres can be measured. In SMFS, the stretching force acts as a denaturant to destabilize the protein, forcing proteins to undergo unfolding along the pulling direction which reveals fundamental information about the conformation of the protein, as well as folding and unfolding dynamics of the protein at the single molecule level.[21–23] Typically a sawtooth pattern is observed in the force–distance curves obtained upon retraction of the AFM tip, with each sawtooth peak corresponding to the unraveling of a portion of the protein molecule.

In the present study, we demonstrate that SMFS can be used to monitor changes in the conformation of β-LG molecules adsorbed at the oil droplet–water interface in response to *in situ* changes in pH. The SMFS measurements are possible only because of the use of a unique sample geometry in which the oil droplets are trapped in the pores of a filtration membrane, allowing us to study a simplified model of milk in which β-LG protein molecules are localized at the oil droplet-water interface. We also compare the conformations of the β-LG molecules adsorbed onto the interface of oil droplets with those measured previously for β-LG molecules adsorbed onto hydrophilic mica surfaces.[24]

Experimental

Emulsion preparation

β-LG was purified from whey protein isolate (New Zealand Dairy Products) by preparative ion chromatography on Q Sepharose (GE Healthcare) using a procedure described by Andrews *et al.*[25] A 2 wt% solution was prepared by dissolving the powdered protein in distilled water at pH 6.8 and then filtering the solution using a 0.8 μm filter (Millex-HV, Millipore Co., Billerica, MA). Oil-in-water emulsions (10% by volume) were prepared by adding 10 mL of soybean oil to 90 mL of β-LG solution. The samples were premixed for 1 min using a high-speed blender (PowerGen 125, Fisher Scientific, Co., Nepean, ON). The protein concentration (0.5 mg ml^{-1}) was chosen as the minimum concentration necessary to obtain a stable emulsion, with a monomodal size distribution of droplets. This indicates a protein concentration that is just sufficient to provide full coverage of the oil droplets. Emulsions were prepared at room temperature using a laboratory-scale, high-pressure homogenizer (Emulsifex C5, Avestin, Ottawa, ON) with two passes at 40 MPa. The emulsions were kept refrigerated at 4 °C for about 24 h, prior to analysis. The particle size distributions of the emulsions were measured using integrated light scattering (Mastersizer, Malvern Instrument, MA).

Droplet immobilization

To perform AFM measurements of biopolymers at the surface of oil droplets in water, it is necessary that the oil droplets be immobilized on a surface. In the present study, the oil droplets were immobilized by mechanically trapping them in the pores of a filtration membrane in which the pore diameter was chosen to be close to the droplet diameter. This is the same approach that has been used successfully for the mechanical trapping of spherical, Gram positive bacteria for use in AFM studies.[26]

100 μL of the oil droplet suspension was incubated at room temperature for 30 min with an Isopore polycarbonate filter membrane (Millipore) with a pore size comparable to the droplet size (pore diameter of 0.4 μm). We note that the oil droplet

diameter (hundreds of nm) is very large compared with the size of the protein molecules (several nm) such that the oil–water interface is essentially flat on length scales comparable to the size of the protein molecules. The filter was then gently rinsed with deionized water to remove the untrapped droplets, and attached to a glass substrate using a small piece of double-sided adhesive tape. The mounted sample was then immediately transferred into the AFM liquid cell containing 20 mM imidazole buffer at pH 6.8. This procedure ensured that droplets remained hydrated and were not subjected to high shear which would dislodge them from the pores, resulting in the trapping of oil droplets in many pores of the filter.

AFM measurements

AFM measurements were performed in contact mode at room temperature using a Multimode AFM with a Nanoscope IV Controller (Digital Instruments, Veeco, Santa Barbara, CA) and V-shaped Si_3N_4 cantilevers with oxide-sharpened tips (Olympus, spring constant of 0.047 N m^{-1}). Contact mode AFM was used so that both AFM images and force–distance curves could be collected on the same area of the sample without changing the AFM cantilever. The spring constants of the cantilevers were determined using the thermal noise technique provided with the instrument software.

AFM images were recorded in both height and deflection modes. The height images provided quantitative information on the sample surface topography. Higher contrast of morphological details was typically observed in the deflection images. Force–distance curves were measured using a z velocity of 500 nm s^{-1}, both on approach and retraction, with an interaction time of ~1 s between the sample and the AFM tip. For all measurements, the maximum loading force was limited to a very low value (< 1 nN). In the force–distance curves shown below, the deflection of the cantilever was subtracted from the measured piezoelectric transducer displacement values which allowed us to plot the applied force *versus* the separation between the AFM tip and the sample surface. For each sample, several images and hundreds of force–distance curves were collected and then analyzed using the Nanoscope IV software (Version 6.13r1, Digital Instruments, Veeco).

All AFM measurements were performed in imidazole buffer. The pH of the fluid above the adsorbed protein layers was changed *in situ* to achieve acidic (pH 2.5) and alkaline (pH 9.0) values, as measured using pH indicator paper, by adding small amounts (typically ~ 30 μl) of hydrochloric acid (0.1 M HCl) or sodium hydroxide (0.1 M NaOH), respectively. This procedure allowed the same region of the protein layer to be investigated using the same AFM tip for different pH values.[24,27]

Analysis of retraction portion of force–distance curves

The mechanical unfolding of the adsorbed β-LG molecules was performed by pulling on the molecules with the AFM tip. For pH values of 2.5 and 6.8, the plot of force *versus* distance for retraction of the tip was characterized by a sawtooth pattern of peaks, which is similar to that observed for the unfolding of a polymer or polypeptide chain.[28] To fit the force *versus* distance data for the unfolding of the β-LG molecules, we used an interpolation formula of the WLC (worm-like chain) model of polymer elasticity[29,30]

$$F(x) = \frac{k_B T}{p}\left[\frac{1}{4(1 - x/L_c)^2} - \frac{1}{4} + \frac{x}{L_c}\right] \quad (1)$$

which is described by two parameters: the persistence length p which is a measure of the polymer chain stiffness, and the contour length L_c. In eqn (1), k_B is Boltzmann's constant and T is the temperature. For all of the sawtooth peaks, the value of p was chosen to be within the range 0.36–0.4 nm which is characteristic of a polypeptide chain and is comparable to the size of a single amino acid residue.[31,32]

For each experimental condition, several hundred force–distance curves were collected and a fit to eqn (1) was performed for each sawtooth peak in the retraction portion of the force–distance curves. Not all of the collected force–distance curves were included in our statistical analysis, and we developed criteria to exclude certain characteristic sawtooth peak patterns. Peaks that occurred within 15 nm of the sample surface (measured from the contact point) were not included to avoid contributions of non-specific interactions between the AFM tip and the sample surface. Force–distance curves with less than three separated peaks were also not included. In addition, there is the possibility that more than one β-LG molecule is attached to the AFM tip. Since the adhesion of multiple molecules results in a different spacing of adjacent unfolding peaks and much higher unfolding forces, all such force–distance curves were excluded from our analysis. Therefore, the data that we included in our analysis most likely originated from the stretching of individual natively folded protein molecules. By applying these criteria for force–distance curve selection, the percentage of successful attempts that showed attachment of a single β-LG molecule to the AFM tip in the force–distance curves was approximately 15% for the mica surface and approximately 10% for the oil droplet surface.

Two different length scales can be obtained from the analysis of the force–distance curves: Δl_c, which represents the difference in contour length between two successive sawtooth peaks, and L_c, which is the contour length of the molecule corresponding to the final sawtooth peak measured upon retraction. Δl_c provides information about the distance between regions with different secondary structure within the molecule or the distance between tethering points within the molecule to the underlying surface. The statistical analysis of several hundred force–distance curves allowed us to obtain average values of Δl_c and L_c and to reliably identify the sawtooth peaks that are characteristic of the mechanical unfolding of the β-LG molecules.

Results

AFM imaging of single oil droplet

In Fig. 1A we show a deflection AFM image recorded in contact mode under 20 mM imidazole buffer at pH 6.8 which shows a relatively large area of the filtration membrane containing many pores. It can be seen that several oil droplets are trapped within pores, as indicated by white arrows. The trapped oil droplets have diameters that range between 0.3 and 0.5 μm. Two large oil droplets can be seen in Fig. 1A (indicated by the black

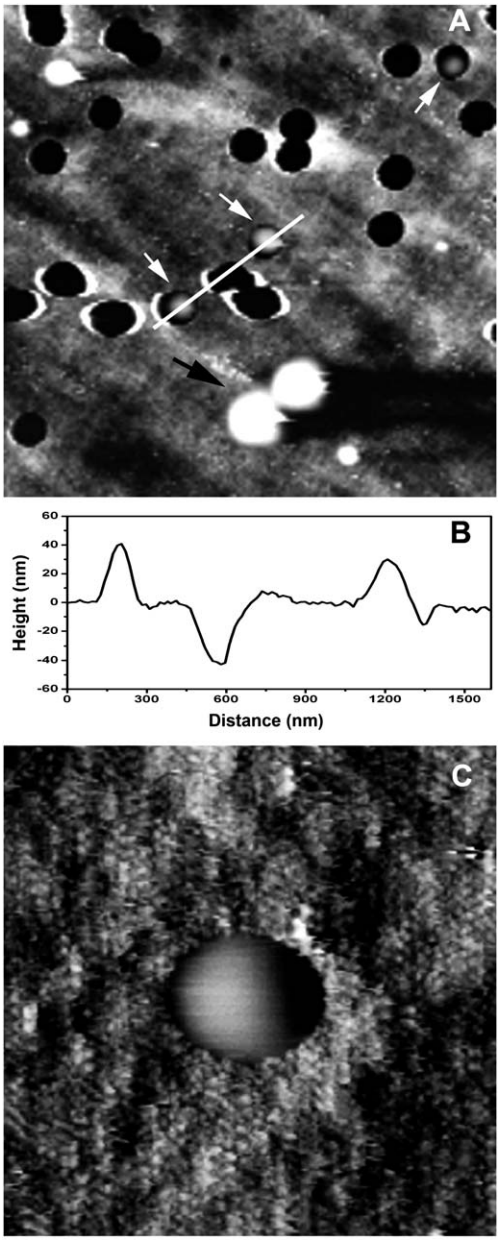

Fig. 1 (A) AFM deflection image of a filtration membrane in which several oil droplets are mechanically trapped in the pores of the membrane (indicated by white arrows). Several other oil droplets can be seen sitting on the solid surface of the membrane (black arrow). The image corresponds to a sample area of 5 × 5 μm. (B) Height profile of the corresponding AFM height image collected along the white solid line shown in part (A). (C) AFM deflection image of a single oil droplet that is mechanically trapped in a pore of the filtration membrane. The image corresponds to a sample area of 1.2 × 1.2 μm.

arrow) and they are probably aggregates of several single small oil droplets which are sitting on top of the filtration membrane surface, and not in the pores. The cross section of the topography along the white line in Fig. 1A is shown in Fig. 1B, and the heights of two trapped oil droplets and the depth of an empty pore can be seen in the line scan. An oil droplet which is well trapped within a pore is shown in Fig. 1C. Typically, trapped oil droplets have heights that are between 10 to 100 nm above the membrane surface. All of the AFM force measurements in the present study were performed on single oil droplets that were well trapped in pores with a droplet height of 20–40 nm above the membrane surface.

AFM force spectroscopy on single oil droplet at different pH values

Representative force–distance curves obtained by stretching β-LG molecules at neutral pH (20 mM imidazole, pH 6.8) are shown in Fig. 2A for the protein on the mica-water interface (upper curve) and for the protein adsorbed at the oil–water interface and measured on the top of the immobilized droplet (lower curve). Each of these curves contains several sawtooth peaks as the tip–sample distance is increased until contact between the tip and the β-LG molecule is broken. The separation between successive peaks was well-defined, suggesting that each peak represents the pulling of a sub-domain of the β-LG molecule. In Fig. 2, it can be seen that the nature of the underlying substrate dramatically affects the conformation and oligomerization of the β-LG molecules at neutral pH. In particular, the distributions of the measured distance Δl_c between peaks and the contour length L_c, which corresponds to the completely stretched state of β-LG molecules, were significantly different for the two surfaces. On the mica surface, the force-extension curves were characterized by large values of Δl_c with an average value of 30 ± 3.7 nm ($n = 900$; Fig. 2B), whereas on the oil droplet surface, Δl_c was a factor of three smaller with an average value of 10.5 ± 2.1 nm ($n = 1100$; Fig. 2C). In Fig. 2D, we show a histogram of the measured contour lengths L_c for the β-LG molecules adsorbed onto the mica surface. There are three peaks in the histogram that are centered at 60 nm, 120 nm, and 180 nm ($n = 300$, Fig. 2D). For the same experimental conditions, the distribution of contour lengths L_c measured for the β-LG molecules adsorbed onto the oil droplet was different, with a large peak centered at 60 nm and a significantly smaller peak centered at 120 nm ($n = 300$; Fig. 2E).

When the pH value of the solution above the adsorbed protein layer was changed *in situ* from neutral pH to an acidic value (pH 2.5), the force-extension curves also consisted of multiple sawtooth peaks as shown in the representative curves in Fig. 3. As in Fig. 2, the upper curve corresponds to β-LG molecules adsorbed onto a mica surface, and the lower curve corresponds to β-LG molecules adsorbed onto an oil droplet. In contrast to the results obtained for neutral pH, the mechanical unfolding of the adsorbed β-LG molecules at acidic pH 2.5 was very similar for the two surfaces. As can be seen in the histograms in Fig. 3B, the average value for Δl_c was 22.2 ± 2.8 nm ($n = 700$) for the force–distance curves collected on the mica surface and Δl_c was 20.3 ± 2.4 nm ($n = 550$, Fig. 3C) for the force–distance curves collected on the oil droplets. The average L_c values were 77.9 ± 19.4 nm ($n = 300$; Fig. 3D) for the mica surface, and 52.8 ± 10 nm ($n = 300$; Fig. 3E) for the oil droplet, which agree to within the experimental uncertainty with the extended length (contour length) of a single β-LG molecule (162 amino acids × 0.36 nm/amino acid = 58.32 nm). This result suggests that the β-LG molecules are adsorbed at the interface as monomers, and that lowering the pH *in situ* produced a stiffer β-LG structure because of the shift to a fully protonated, positively charged protein.

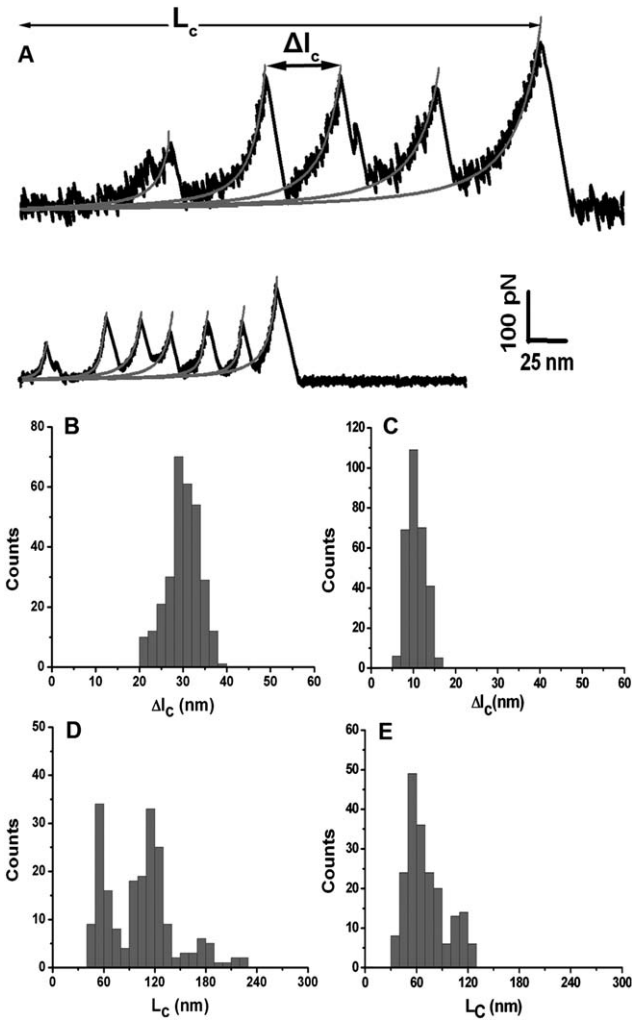

Fig. 2 (A) Representative curves of the retraction portion of AFM force–distance curves, recorded between the AFM tip and β-LG molecules adsorbed onto a mica surface (upper curve) and adsorbed onto an oil droplet surface (lower curve). In both cases, the samples were maintained under imidazole buffer at pH 6.8. Both curves show a sawtooth pattern of peaks that corresponds to the mechanical unfolding of β-LG molecules. The smooth curves correspond to best fits of the data to eqn (1). We also show histograms of various quantities measured from hundreds of force–distance curves collected for β-LG molecules on the two surfaces. (B) and (D): distance between sawtooth peaks Δl_c and contour length L_c for β-LG molecules on the mica surface; and (C) and (E): distance between sawtooth peaks Δl_c and contour length L_c for β-LG molecules on the oil droplet surface.

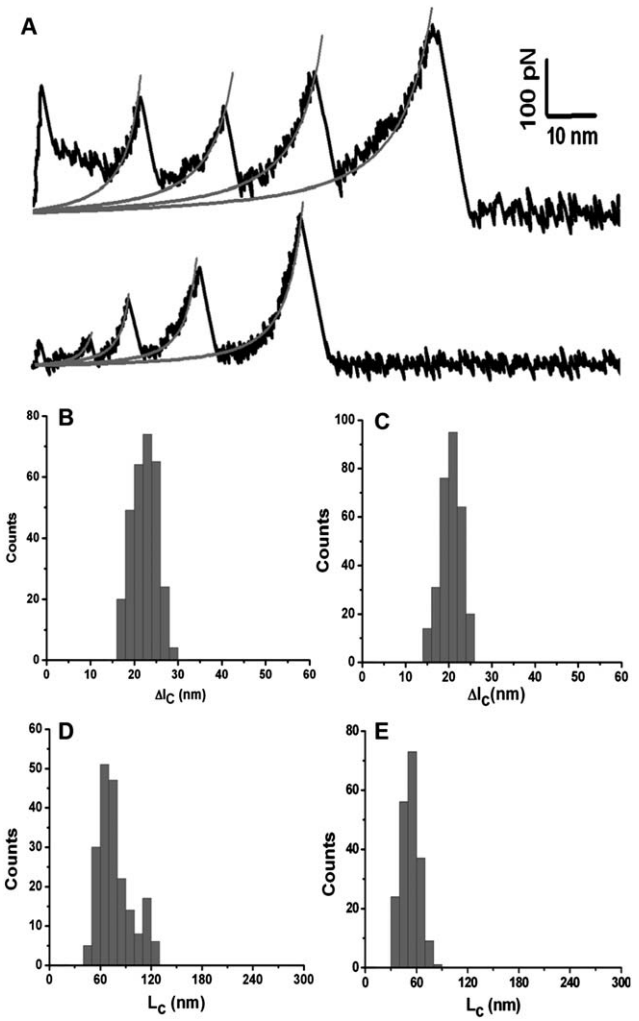

Fig. 3 (A) Representative curves of the retraction portion of AFM force–distance curves, recorded between the AFM tip and β-LG molecules at the mica surface (upper curve) and the oil droplet surface (lower curve) after adjusting the pH *in situ* to 2.5. Both curves show a sawtooth pattern of peaks that corresponds to the mechanical unfolding of β-LG molecules. The smooth curves correspond to best fits of the data to eqn (1). We also show histograms of various quantities measured from hundreds of force–distance curves collected for β-LG molecules on the two surfaces. (B) and (D): distance between sawtooth peaks Δl_c and contour length L_c for β-LG molecules on the mica surface; and (C) and (E): distance between sawtooth peaks Δl_c and contour length L_c for β-LG molecules on the oil droplet surface.

When the pH of the solution was changed *in situ* from pH 6.8 to an alkaline value (pH 9.0), the force–distance curves collected on the β-LG molecules on both the oil droplet and mica surfaces were significantly different from those measured for pH 2.5 and 6.8. For both surfaces at pH 9.0, a significant repulsion between the AFM tip and the adsorbed protein layer was observed during the approach of the AFM tip to the sample surface, with the repulsive force increasing approximately exponentially with decreasing tip–sample distance (Fig. 4A). For the oil droplet surface, a small adhesion between the tip and the β-LG molecules was observed during the retraction of the tip from the surface (lower curve in Fig. 4A); no such adhesion was observed for the mica surface. The distance over which a substantial repulsive force was experienced by the AFM tip differed significantly for the two surfaces: ~40 nm for β-LG molecules adsorbed onto the hydrophobic oil droplet surface, *versus* ~100 nm for β-LG molecules adsorbed onto the hydrophilic mica surface, as reported in our previous study.[24]

Discussion

At the outset, we expect that, because the mica surface is hydrophilic, the conformation of the β-LG molecules adsorbed onto the hydrophilic mica–water interface should be similar to

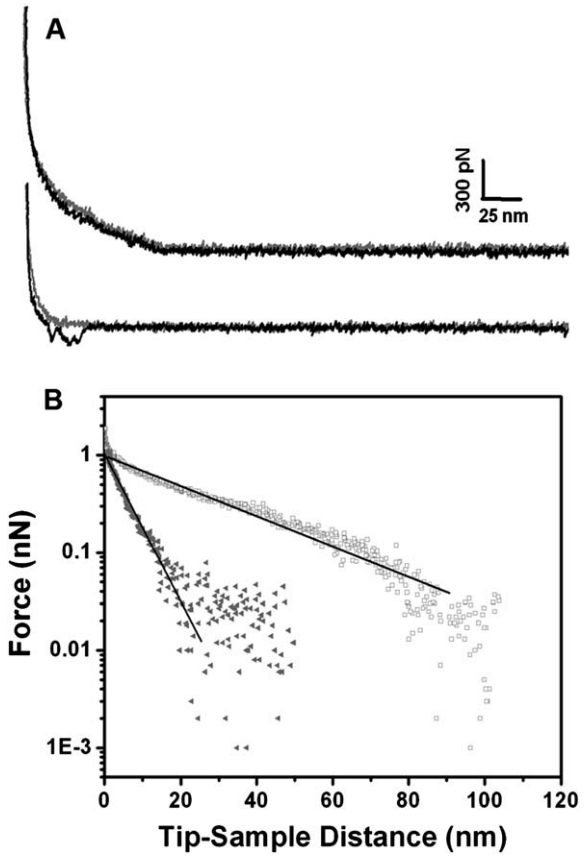

Fig. 4 (A) Representative curves of the approach and retraction portions of AFM force–distance curves, recorded between the AFM tip and β-LG molecules on the mica surface (upper curve) and the oil droplet surface (lower curve), after adjustment to pH 9.0. (B) Semi-logarithmic plot of force *versus* tip–sample distance for β-LG molecules adsorbed onto a mica surface (open squares) and an oil droplet surface (solid triangles). The straight lines correspond to the best fits of the data to eqn (2).

that in solution. In contrast, we expect that the conformation of the β-LG molecules adsorbed onto the hydrophobic oil–water interface could be significantly different. In addition, since β-LG molecules contain many charged groups, the structure and properties of the molecules depend strongly on the pH and ionic strength of the surrounding media. In particular, it has been established that the emulsifying properties of β-LG depend on pH.[33,34] Because of this, it is useful to compare the single molecule force spectroscopy (SMFS) results obtained for the β-LG molecules adsorbed onto the hydrophobic oil–water and hydrophilic mica-water interfaces at different values of pH.

Adsorbed β-LG molecules at neutral pH 6.8

At neutral pH (pH 6.8), the force–distance curves obtained by pulling on the adsorbed β-LG molecules were significantly different for the protein on mica and on the oil droplet. For example, the β-LG molecules adsorbed onto the oil droplet surface unfold with a smaller applied force (~100 pN) than the force (~180 pN) that is needed to unfold the molecules when they are adsorbed onto the mica surface (*cf.* Fig. 2). Despite this difference, the measured forces that are required to mechanically unfold β-LG molecules on both surfaces are within the range of values reported for the mechanical unfolding at comparable pulling speeds of individual units of modular β-sheet proteins, such as titin (80–300 pN)[35–37] or tenascin (~137 pN),[38] and are significantly larger than those typically observed for the unfolding of α-helical proteins such as spectrin (15–25 pN)[39] or lysozyme (64 pN).[40] This result is reasonable, given the β-sheet character (52% β-sheet and 10% α-helix[38,33]) of the β-LG molecules in solution, which is thought to be comparable for β-LG molecules at the oil–water interface.[12,41] In addition, our measurement of a smaller unfolding force for the oil–water interface is consistent with differential scanning calorimetry data which showed a smaller enthalpy for the protein at the oil–water interface than in solution.[2]

The differences between the force–distance curves obtained for the protein on the mica and oil droplet surfaces can also be seen in the measured distances Δl_c between successive sawtooth peaks and the contour length L_c as shown in Fig. 2A. By fitting the shape of each sawtooth peak to the WLC model using eqn (1), the effective contour length of the polypeptide chain between the sawtooth peak and the sample surface can be determined. For β-LG molecules on the oil droplet surface, we find that there is a difference of about $\Delta l_c = 10.5$ nm between the L_c values obtained for successive peaks. This value of Δl_c corresponds to a stretched length of polypeptide that is 29 amino acids (aa) long, assuming a persistence length of 0.36 nm. In contrast, the distance between successive peaks Δl_c for β-LG molecules on the mica surface is approximately three times larger (~30 nm, corresponding to 83 aa). This value of Δl_c is similar to the length of single immunoglobulin domains for a β-sheet protein.[36] These results suggest that the β-LG molecules adopt very different conformations on the two surfaces at pH 6.8 with small secondary structure domains on the oil droplet and large domains on the mica surface. It is worth pointing out that if the differences between the results obtained on the mica and oil droplet surfaces were just due to the deformation of the oil droplet surface upon retraction, the values of L_c and Δl_c would be larger on the oil droplet surface, which is not consistent with our data.

These differences between the force–distance curves obtained for the β-LG molecules on the mica and oil droplet surfaces can be understood qualitatively in terms of the driving forces for protein adsorption. It has been found that proteins adsorb strongly and less reversibly at hydrophobic surfaces than at hydrophilic surfaces.[42,43] This behavior was illustrated clearly in two studies that used gradient hydrophobic surfaces: a study by Prime and Whitesides[44] that showed that proteins adsorb more strongly as the hydrophobicity of the surface is increased; and a study by Elwing *et al.*[45] that showed that exchange of adsorbed protein molecules with surfactants in the bulk aqueous phase is generally reduced with an increasing degree of hydrophobicity of the surface. These results can be attributed to a greater degree of unfolding of proteins upon adsorption onto hydrophobic surfaces.[43] In addition, these data are consistent with the hypothesized upside down calyx structure within the β-LG molecules due to the formation of breaks in β-sheets at the oil–water interface. The upside down calyx provides a hydrophobic driving force for the adsorption of the protein

onto the oil droplet surface. Electrostatic interactions are more important between proteins and hydrophilic surfaces, especially for globular proteins such as β-LG molecules, which may undergo very little change in conformational structure upon adsorption.[42,43,46] The difference observed in the present study between the conformations of β-LG molecules adsorbed onto the mica and oil droplet surfaces implies very different extents of denaturation and oligomerization upon adsorption. The conformation of the adsorbed protein will, in general, depend on the concentration of the protein in the emulsion.[47] If there is an excess of protein compared with that required for monolayer coverage of the oil droplets, the β-LG molecules adsorb onto the mica surface with little change from their native conformation.[47] The conformation of the adsorbed β-LG molecules can then change slightly with time, as more ordered structural units are removed and intermolecular bonds are formed.[47] If the protein concentration is less than that required for monolayer coverage of the oil droplets, there is a lower packing density of the adsorbed molecules that provides more space for each protein molecule to spread out at the oil–water interface, increasing the stability of the emulsion. Our observation of significantly smaller secondary structure domains for β-LG molecules adsorbed onto oil droplet surfaces indicates a higher degree of denaturation of the molecules at the oil–water interface. Although we did not measure the surface coverage of the β-LG molecules directly, we can infer that the surface coverage is larger for the mica surface since the percentage of successful attempts that showed attachment of a single β-LG molecule to the AFM tip was larger for the mica surface (∼15%) than for the oil droplet surface (∼10%).

It is also useful to compare the contour length L_c values obtained from SMFS measurements of β-LG on the mica and oil droplet surfaces. For the mica surface, in addition to the distinct peak in the histogram of contour length L_c values at 60 nm which corresponds to single β-LG molecules (162 aa × 0.36 nm/aa = 58.32 nm), there is a significant peak in the histogram of contour length L_c values at 120 nm shown in Fig. 2D. The 120 nm value corresponds to the length of β-LG dimers which is the dominant structure of β-LG molecules in solution at neutral pH. There is also a small distribution of L_c values centred about 180 nm indicating a small presence of trimeric β-LG structures. These observations, which correspond closely to the β-LG structure observed in solution, strongly suggest that the β-LG molecules experience only minimal changes in their conformation upon adsorption to the hydrophilic mica surface. In contrast, for β-LG molecules adsorbed onto an oil droplet surface through high pressure homogenization, the distribution of contour length L_c values shown in Fig. 2E shows the predominant presence of single β-LG molecules or monomers, with only a small amount of dimers present.

To help in understanding the change in conformation of β-LG upon adsorption at the oil–water interface at neutral pH, as inferred from the SMFS results, we have examined the hydropathy and secondary structure propensity of the β-LG molecule. The hydropathy of each amino acid in the molecule can be specified using the Kyte-Doolittle method.[48] The secondary structure propensity is a measure of the likelihood that an amino acid will form an α-helix or β-sheet, using the Chou-Fasman scale,[49] and we can use this as a guide to predict possible transitions in the secondary structure of the molecules. The results of the hydropathy and secondary structure propensity analysis for the primary sequence of β-LG at neutral pH are shown in Fig. 5A using a window average of 7 residues. Positive (negative) values of the secondary structure propensity indicate a higher β-sheet (α-helix) propensity. In Fig. 5B is shown the secondary structure of β-LG in solution (pdb code 2GJ5) that is colored according to the secondary structure propensity shown in Fig. 5A. In this structure, β-strands 6 and 8 sandwich β-strand 7 with high β-sheet propensity in the core of the protein, whereas β-strands 2, 3 and 4 lie at the surface of the protein and show high α-helical propensity. This suggests that strands 2, 3, and 4 may undergo a β-to-α transition upon binding to a surface. By analyzing the hydropathy of each of the surface β-strands with no window averaging, it is apparent that α-helices formed in these regions would be amphiphilic, as shown in Fig. 5C. The hydropathy of strands 2, 3 and 4 are periodic, with periods of 3, 4 and 5 amino acids respectively. On average, these values are close to the number of amino acids per turn in an α-helix (3.6 amino acids per turn), which suggests that the α-helices (if they do form) could be organized with their axes aligned parallel to the oil–water interface with the hydrophobic residues in the oil and the hydrophilic residues in the water.

In the native state of β-LG, 27 of the 162 amino acids, or 17%, form α-helices. If the three surface β-strands were to undergo a transition to α-helices, 55 of the 162 amino acids, or 34%, would form α-helices. This increase in α-helix content, with a corresponding decrease in β-sheet content, agrees with previous studies of changes in conformation upon adsorption of β-LG to the oil–water interface.[13] These findings are consistent with several previous studies in which the environmental conditions were changed to promote the β-sheet to α-helix transition in β-LG. Such a transition has been observed in β-LG upon lowering to pH 2 and introducing 2,2,2-trifluoroethanol.[50] The authors of this study deduced through NMR analysis that, although the core β-sheet remained intact, the characteristic peaks of β-strands 2, 3 and 4 were missing and likely assumed a helical conformation. In the folding of β-LG, the first step is likely the formation of the core β-sheet. Before the other strands are formed, it is possible that their high α-helical propensity allows for a folding intermediate with higher α-helix content in these regions.[51,52]

Adsorbed β-LG molecules at acidic pH 2.5

Upon changing the pH value *in situ* from 6.8 to an acidic value of 2.5, mechanical stretching of the β-LG molecules resulted in force–distance curves that were almost identical for the mica and oil droplet surfaces, and these curves were substantially different from those measured at neutral pH. The oligomerization of β-LG molecules on the mica surface at neutral pH is not present at pH 2.5. For both surfaces, larger forces are required to unfold the secondary structure domains relative to those measured at neutral pH: ∼ 260 pN for β-LG molecules adsorbed onto the mica surface and ∼ 200 pN for β-LG molecules adsorbed onto the oil droplet surface.

The β-LG molecules, which are positively charged at pH 2.5, interact strongly with each other and with the mica surface,

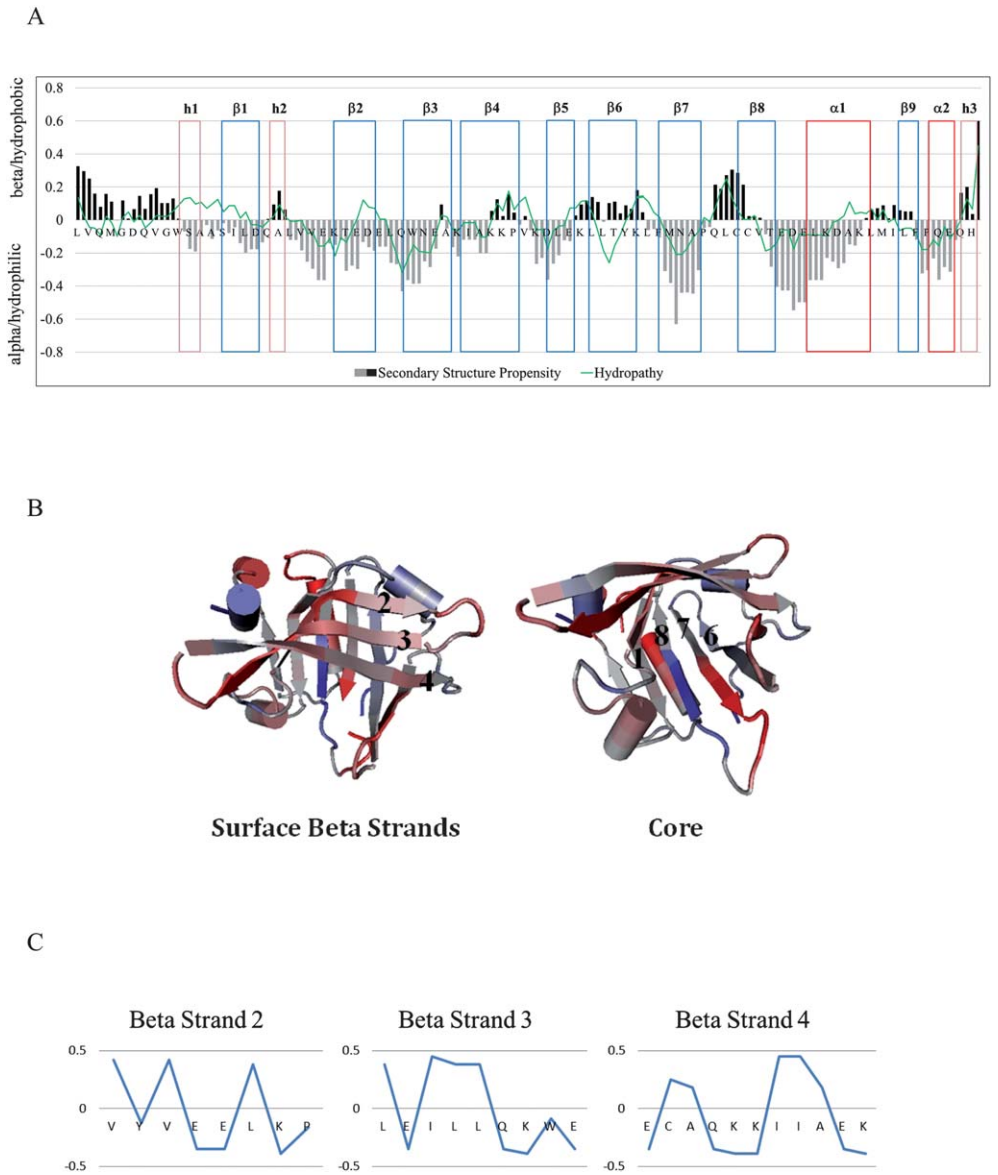

Fig. 5 (A) Plot of hydropathy (green curve) and secondary structure propensity (bars) for the primary amino acid sequence of β-LG, using an averaging window of 7 residues for both quantities. Positive (negative) values of the hydropathy index correspond to hydrophilic (hydrophobic) residues, and are calculated by dividing the Kyte-Doolittle score by ten. Positive (negative) values of the secondary structure propensity index correspond to a propensity for β-sheets (α-helices), and are calculated by taking the difference between the Chou-Fasman β-sheet and α-helix scores. The blue rectangles indicate β-strands and are labeled from β1 to β9, red rectangles indicate α-helices α1–α2 and pink rectangles 3–10 helices h1–h3; (B) Ribbon diagrams of the β-LG (pdb code 2GJ5) molecule showing the propensity of β-strands (blue) and α-helices (red), with the beta strands labeled as in (A). (C) Hydropathy of surface beta strands 2, 3 and 4 shown without window averaging, which reveals a periodicity that is suggestive of amphipathic helices.

which is negatively charged at pH 2.5.[24] In addition, β-LG molecules at acidic pH values have a lower emulsifying capacity and surface activity than at neutral pH, even though their surface hydrophobicity is greater at acidic pH values.[33,34] It is thought that this is because the molecules are more difficult to denature at low pH. As shown in Fig. 3B and 3C, the number of amino acids involved in structural domains was well-defined by narrow distributions with similar values for both surfaces: ~61 aa (22 nm/0.36 nm) for β-LG molecules on mica, and ~56 aa (20 nm/0.36 nm) for β-LG molecules adsorbed onto an oil droplet surface. These values are significantly different from those measured for β-LG molecules for the two surfaces at neutral pH. Also the histogram of the contour length L_c values shown in Fig. 3D and 3E show that there are predominantly monomers present (peak at 60 nm Fig. 3D and 3E) with only a small amount of dimers present on the mica surface (peak at 120 nm Fig. 3D). This result is consistent with the dissociation of β-LG dimers into single molecules in bulk solutions with pH < 3.5.[11] We note that the changes observed in the force–distance curves collected on the mica and the oil droplet surfaces by changing the pH from 6.8 to 2.5 were reversible: by changing the pH *in situ* back to the neutral value of pH 6.8, we measured force–distance curves that were very similar to those measured originally at neutral pH.

Adsorbed β-LG molecules at alkaline pH 9.0

Upon changing the pH value *in situ* from 6.8 to an alkaline value of 9.0, the force–distance curves were dramatically altered on both the mica and oil droplet surfaces. In particular, the approach and retraction force–distance curves obtained at pH 9.0 are essentially identical and are well described by a large repulsion between the adsorbed β-LG layer and the AFM tip (Fig. 4A). This behavior manifests itself as an exponential dependence of the repulsive force experienced by an AFM tip on the distance between the tip and the sample. Previous studies have shown a similar interaction between an AFM tip and polypeptides and polymers grafted onto a solid surface due to steric repulsion.[53,54] In their study of human nucleoporin Nup153 molecules covalently tethered to gold nanodots,[53] Lim *et al.* observed a repulsion that was similar to that observed in the present study for β-LG molecules adsorbed onto the oil droplet. In their AFM study of PEO-PS block copolymers grafted to a mica surface under various solvents, O'Shea and coworkers[54] investigated the repulsion between the AFM tip and the grafted polymer layer, and they observed force–distance curves that were very similar to those obtained in the present study for β-LG molecules adsorbed onto mica surfaces. We note that in the present study part of the large repulsion force between the AFM tip and the β-LG molecules is due to electrostatic repulsion since both the tip and the molecules are negatively charged at pH 9.0. However, the force–distance curves should not be significantly affected by the electrostatic repulsion for two reasons: (1) the charge on the β-LG molecules at pH 9.0 is small (two negative charges per molecule); and (2) the magnitude of the repulsive force is much larger than that expected for electrostatic repulsion effects, as has been reported in a similar study on charged poly (*N*,*N*-dimethylacrylamide) (PDMA) brushes on latex particles.[55] Because of this, we neglect electrostatic effects in the following analysis of the force–distance curves in Fig. 4A.

The Alexander-de Gennes theory[56] for the force acting between two surfaces bearing polymer brushes in good solvents has been shown to be a reasonable description of AFM force–distance curves for polypeptide and polymer brushes and we use this theory to interpret the data obtained for pH 9.0 in the present study. The basis of the Alexander-de Gennes theory is the assumption that the repulsive interaction between parallel surfaces bearing grafted polymer layers and separated by a distance D is a combination of the osmotic repulsion caused by the increase in polymer concentration as the surfaces are brought together, and the decrease in elastic energy of the polymer chains as they are compressed. We have used a variation of the Alexander-de Gennes theory in which only one surface is coated by a polymer brush (which is appropriate for AFM experiments).[53,54,56–59] In this theory, which essentially ignores the strong osmotic repulsive forces resulting from the compression of the chains, the force F is given by:[53]

$$F(D) = \frac{100\ \pi\ R_{eff}\ D}{s^3} k_B T e^{-2\pi D/L} \qquad (2)$$

where s is the mean distance between the tethering points of the polymer brush, D is the distance between the surfaces, k_B is Boltzmann's constant, T is the temperature, and L is the equilibrium thickness of the brush layer. R_{eff} is the effective radius of curvature which is given by $R_{eff} = (R_{tip} \times R_{surface})/(R_{tip} + R_{surface})$, and R_{tip} and $R_{surface}$ are the radii of curvature of the AFM tip and the oil droplet, respectively (for the β-LG protein layer on the mica surface, $R_{eff} = R_{tip}$). Eqn (2) is valid for separation distances D satisfying $0.2 < D/2L < 0.9$.

To evaluate the values of L and s for our experiment, we fit the AFM approach force–distance curves such as those shown in Fig. 4A to eqn (2). The corresponding best fit curves for the mica and oil droplet surfaces are plotted as the logarithm of the force *versus* tip–sample distance in Fig. 4B. The slope of the best fit to the data on the semi-logarithmic plot is a measure of the inverse of the equilibrium brush thickness L (*cf.* eqn (2)). Using a tip radius of $R_{tip} = 20$ nm, the values obtained by averaging 30 force–distance curves for each surface resulted in $L = 35.5 \pm 6.7$ nm and $s = 19.3 \pm 3.2$ nm for the oil droplet, and $L = 135.5 \pm 8$ nm and $s = 15.3 \pm 3.5$ nm for the mica surface.

The best fit values of the average spacing s of the β-LG molecules on the two surfaces are the same to within the uncertainty associated with the fitting procedure, and are large compared with the size of the β-LG monomer at neutral pH (~3.6 nm).[60] Most strikingly, we obtain best fit values for the equilibrium brush thicknesses L for the two surfaces that differ by a factor of four, which implies very different conformations of the β-LG molecules on the two surfaces at pH 9.0. We note that the large value of L for β-LG molecules adsorbed onto the mica surface is similar to that observed for AFM force–distance curves for grafted PEO layers.[54] In contrast, the small value of L for β-LG molecules adsorbed onto the oil droplet surface allows for the observation of small peaks in the retraction part of the force–distance curves, as shown in the lower curve of Fig. 4A, corresponding to a short-range adhesion which is similar to the result obtained by Lim *et al.* for cNup153 proteins tethered to gold nanodots.[53]

We note that, unlike the reversible transitions observed in β-LG conformation upon changing the pH value from 6.8 to 2.5 and back to 6.8, β-LG molecules undergo an irreversible unfolding transition upon changing the pH from 6.8 to 9.0, with global disruption of both secondary and tertiary structures.[60,61]

Conclusions

We have demonstrated that single molecule force spectroscopy (SMFS) can be used to reveal significant differences in the conformation of protein molecules adsorbed onto hydrophilic and hydrophobic surfaces at different pH values. In particular, the present study provides a new experimental window on the determination of changes that occur in the conformation of β-LG molecules upon adsorption to the oil–water interface, which complements the determination of secondary structure using more conventional techniques that are technically challenging for oil-in-water emulsions. By mechanically trapping small oil droplets in the pores of a filtration membrane, we have created an ideal sample geometry for performing the SMFS measurements on β-LG molecules at the oil–water interface while allowing *in situ* changes in the pH value of the surrounding buffer.

The SMFS results obtained in the present study for β-LG molecules on the hydrophobic oil droplet surface are compared to our previous results for the same molecules on the hydrophilic

mica surface, and we observe large differences. At neutral pH, we observe large differences, not only in the pulling force required to fully extend the molecules, but also very significant differences in the spacing between sawtooth peaks in the force–distance curves and the oligomerization of the molecules. This result is consistent with a significant rearrangement of the β-LG molecules at the hydrophobic oil droplet surface. In contrast to the results obtained for pH 6.8, the mechanical unfolding of the adsorbed β-LG molecules at pH 2.5 was very similar for the two surfaces. For pH 9.0, we find that, for both surfaces, there is an irreversible change in the conformation of the β-LG molecules with a strong repulsion measured between the AFM tip and the β-LG molecules that prevents the β-LG molecules from adhering to the AFM tip and being stretched mechanically. We have interpreted the data collected at pH 9.0 quantitatively in terms of the Alexander-de Gennes polymer brush theory, and we find that the characteristic repulsion distance and the corresponding equilibrium brush height is smaller for the hydrophobic surface by a factor of four.

The present study shows that SMFS can be used to characterize differences in the conformation and structural changes of protein molecules adsorbed onto different surfaces and under different environmental conditions. Further work is needed to relate the conformational information obtained from SMFS to other techniques that are used for the determination of the secondary structure of proteins.

Acknowledgements

The authors gratefully acknowledge financial support from the Advanced Foods and Materials Network (AFMnet), the Natural Sciences and Engineering Research Council of Canada, and the Canadian Foundation for Innovation. MC and JRD acknowledge support from the Canada Research Chairs (CRC) program.

References:

1 J. A. Hunt and D. G. Dalgleish, *J. Food Sci.*, 1995, **60**, 1120–1123.
2 M. Corredig and D. G. Dalgleish, *Colloids Surf., B*, 1995, **4**, 411–422.
3 V. Hlady and J. Buijs, *Curr. Opin. Biotechnol.*, 1996, **7**, 72–77.
4 K. Nakanishi, T. Sakiyama and K. Imamura, *J. Biosci. Bioeng.*, 2001, **91**, 233–244.
5 L. Sawyer, *β-Lactoglobulin, in Advanced Dairy Chemistry*, 3rd ed.; P. F. Fox, P. L. H. McSweeney, ed.; Kluwer Academic/Plenum Publishers: New York, 2003; Vol. 1 (Proteins), Part B, pp 319–386.
6 E. Dickinson and G. Stainsby, *Colloids in Food*; Chapman and Hall: London, 1982.
7 M. Z. Papiz, L. Sawyer, E. E. Eliopoulos, A. C. North, J. B. Findlay, R. Sivaprasadarao, T. A. Jones, M. E. Newcomer and P. J. Kraulis, *Nature*, 1986, **324**, 383–385.
8 S. Brownlow, J. H. Morais Cabral, R. Cooper, D. R. Flower, S. J. Yewdall, I. Polikarpov, A. C. T. North and L. Sawyer, *Structure*, 1997, **5**, 481–495.
9 S. Uhrinova, D. Uhrin, H. Denton, M. Smith, L. Sawyer and P. N. Barlow, *J. Biomol. NMR*, 1998, **12**, 89–107.
10 M. D. Perez and M. Calvo, *J. Dairy Sci.*, 1995, **78**, 978–988.
11 R. D. Fugate and P. S. Song, *Biochim. Biophys. Acta*, 1980, **625**, 28–42.
12 Y. Fang and D. G. Dalgleish, *J. Colloid Interface Sci.*, 1997, **196**, 292–298.
13 F. A. Husband, M. J. Garrood, A. R. Mackie, G. R. Burnett and P. J. Wilde, *J. Agric. Food Chem.*, 2001, **49**, 859–866.
14 S.-H. Lee, T. Lefèvre, M. Subirade and P. Paquin, *J. Agric. Food Chem.*, 2007, **55**, 10924–10931.
15 M. M. Sakuno, S. Matsumoto, S. Kawai, K. Taihei and Y. Matsumura, *Langmuir*, 2008, **24**, 11483–11488.
16 K. Gekko and S. N. Timasheff, *Biochemistry*, 1981, **20**, 4667–4676.
17 A. Priev, A. Almagor, S. Yedgar and B. Gavish, *Biochemistry*, 1996, **35**, 2061–2066.
18 V. Vagenende, M. G. S. Yap and B. L. Trout, *Biochemistry*, 2009, **48**, 11084–11096.
19 J. Zhai, A. J. Miles, L. K. Pattenden, T.-H. Lee, M. A. Augustin, B. A. Wallace, M.-I. Aguilar and T. J. Wooster, *Biomacromolecules*, 2010, **11**, 2136–2142.
20 G. Binning, C. F. Quate and Ch. Gerber, *Phys. Rev. Lett.*, 1986, **56**, 930–933.
21 T. E. Fisher, A. F. Oberhauser, M. Carrion-Vazquez, P. E. Marszalek and J. M. Fernandez, *Trends Biochem. Sci.*, 1999, **24**, 379–384.
22 D. J. Brockwell, *Curr. Nanosci.*, 2007, **3**, 3–15.
23 J. M. Fernandez and H. Li, *Science*, 2004, **303**, 1674–1678.
24 A. Touhami and J. R. Dutcher, *Soft Matter*, 2009, **5**, 220–229.
25 A. T. Andrew, M. D. Taylor and A. J. Owen, *J. Chromatogr., A*, 1985, **348**, 177–185.
26 S. Kasas and A. Ikai, *Biophys. J.*, 1995, **68**, 1678–1680.
27 F. Ahimou, F. A. Denis, A. Touhami and Y. F. Dufrêne, *Langmuir*, 2002, **18**, 9937–9941.
28 A. Janshoff, M. Neitzert, Y. Oberdörfer and H. Fuchs, *Angew. Chem., Int. Ed.*, 2000, **39**, 3213–3237.
29 C. Bustamante, J. F. Marko, E. D. Siggia and S. Smith, *Science*, 1994, **265**, 1599–1600.
30 J. F. Marko and E. D. Siggia, *Macromolecules*, 1995, **28**, 8759–8770.
31 M. Rief, M. Gautel, F. Oesterhelt, J. M. Fernandez and H. E. Gaub, *Science*, 1997, **276**, 1109–1112.
32 C. Bouchiat, M. D. Wang, J.-F. Allemand, T. Strick, S. M. Block and V. Croquette, *Biophys. J.*, 1999, **76**, 409–413.
33 M. Shimizu, M. Saito and K. Yamauchi, *Agric. Biol. Chem.*, 1985, **49**, 189–194.
34 K. Yamauchi, M. Shimizu and T. Kamiya, *J. Food Sci.*, 1980, **45**, 1237–1242.
35 H. Li, M. Carrion-Vazquez, A. F. Oberhauser, P. E. Marszalek and J. M. Fernandez, *Nat. Struct. Biol.*, 2000, **7**, 1117–1120.
36 D. J. Brockwell, G. S. Beddard, E. Paci, D. K. West, P. D. Olmsted, D. A. Smith and S. E. Radford, *Biophys. J.*, 2005, **89**, 506–519.
37 M. Rief, M. Gautel, A. Schemmel and H. E. Gaub, *Biophys. J.*, 1998, **75**, 3008–3014.
38 A. F. Oberhauser, P. E. Marszalek, H. P. Erickson and J. M. Fernandez, *Nature*, 1998, **393**, 181–185.
39 M. Rief, J. Pascual, M. Saraste and H. E. Gaub, *J. Mol. Biol.*, 1999, **286**, 553–561.
40 G. Yang, C. Cecconi, W. A. Baase, I. R. Vetter, W. A. Breyer, J. A. Haack, B. W. Matthews, F. W. Dahlquist and C. Bustamante, *Proc. Natl. Acad. Sci. U. S. A.*, 2000, **97**, 139–144.
41 D. C. Clark and L. J. Smith, *J. Agric. Food Chem.*, 1989, **37**, 627–633.
42 M. Malmsten, *J. Colloid Interface Sci.*, 1998, **207**, 186–199.
43 E. Dickinson, *Colloids Surf., B*, 1999, **15**, 161–176.
44 K. L. Prime and G. M. Whitesides, *Science*, 1991, **252**, 1164–1167.
45 H. Elwing, S. Welin, A. Askendal, U. Nilsson and I. Lundström, *J. Colloid Interface Sci.*, 1987, **119**, 203–210.
46 W. Norde, *Adv. Colloid Interface Sci.*, 1986, **25**, 267–340.
47 D. G. Dalgleish, *Trends Food Sci. Technol.*, 1997, **8**, 1–6.
48 J. Kyte and R. F. Doolittle, *J. Mol. Biol.*, 1982, **157**, 105–132.
49 P. Y. Chou and G. D. Fasman, *Biochemistry*, 1974, **13**, 211–222.
50 K. Kuwata, M. Hoshino, S. Era, C. A. Batt and Y. Goto, *J. Mol. Biol.*, 1998, **283**, 731–739.
51 K. Sakurai, T. Konuma, M. Yagi and Y. Goto, *Biochim. Biophys. Acta, Gen. Subj.*, 2009, **1790**, 527–537.
52 D. Hamada, Y. Kuroda, T. Tanaka and Y. Goto, *J. Mol. Biol.*, 1995, **254**, 737–746.
53 R. Y. H. Lim, N.-P. Huang, J. Köser, J. Deng, K. H. A. Lau, K. Schwarz-Herion, B. Fahrenkrog and U. Aebi, *Proc. Natl. Acad. Sci. U. S. A.*, 2006, **103**, 9512–9517; R. Y. H. Lim, B. Fahrenkrog, J. Köser, K. Schwarz-Herion, J. Deng and U. Aebi, *Science*, 2007, **318**, 640–643 [plus supplementary info from PNAS].
54 S. J. O'Shea, M. E. Welland and T. Rayment, *Langmuir*, 1993, **9**, 1826–1835.
55 D. Goodman, J. N. Kizhakkedathu and D. E. Brooks, *Langmuir*, 2004, **20**, 2333–2340.

56 P. G. de Gennes, *Adv. Colloid Interface Sci.*, 1987, **27**, 189–209.
57 J. N. Israelachvili, *Intermolecular and Surface Forces* (Academic, London, 1995).
58 H. G. Brown and J. H. Hoh, *Biochemistry*, 1997, **36**, 15035–15040.
59 H. J. Butt, M. Kappl, H. Mueller, R. Raiteri, W. Meyer and J. Rühe, *Langmuir*, 1999, **15**, 2559–2565.
60 H. A. McKenzie and W. H. Sawyer, *Nature*, 1967, **214**, 1101–1104.
61 H. L. Casal, U. Köhler and H. H. Mantsch, *Biochim. Biophys. Acta, Protein Struct. Mol. Enzymol.*, 1988, **957**, 11–20.

